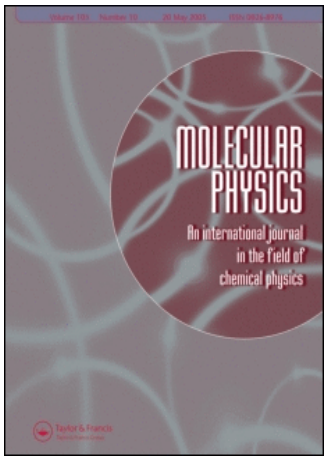

Molecular Physics
An International Journal in the Field of Chemical Physics
Publication details, including instructions for authors and subscription information:
http://www.informaworld.com/smpp/title~content=t713395160

Monte Carlo study of rod-like molecules

Carlos Vega [a]; Daan Frenkel [ab]
[a] F.O.M. Institute for Atomic and Molecular Physics. Amsterdam. The Netherlands
[b] Physical Chemistry Department, Chemistry Faculty, Complutense University. Madrid. Spain

Online Publication Date: 20 June 1989
To cite this Article: Vega, Carlos and Frenkel, Daan , (1989) 'Monte Carlo study of rod-like molecules', Molecular Physics, 67:3, 633 - 650
To link to this article: DOI: 10.1080/00268978900101331
URL: http://dx.doi.org/10.1080/00268978900101331

MOLECULAR PHYSICS, 1989, VOL. 67, NO. 3, 633–650

Monte Carlo study of rod-like molecules
A test of perturbation theory for the Kihara model

by CARLOS VEGA and DAAN FRENKEL†
F.O.M. Institute for Atomic and Molecular Physics, P.O. Box 41883,
1009 DB Amsterdam, The Netherlands

(*Received 20 December 1988; accepted 24 January 1989*)

We report a Monte Carlo study of fluids of linear, rod like molecules interacting either through a Kihara potential, or its soft repulsive potential counterpart. The internal energy, equation of state and a number of static correlation functions were obtained from the simulation. We compare the MC results with the predictions based on a perturbation theory due to Boublik.

1. Introduction

The non-central interactions of molecular fluids can be modeled in several ways. Best known among these is probably the multi-centre (interaction site) model [1]. A rather different model that can be used is the Kihara potential. In the latter model the intermolecular interaction between two molecules is assumed to depend exclusively on the shortest distance ρ between the convex hard cores of the molecules (e.g. spherocylinders or ellipsoids). Although the Kihara potential is probably not particularly useful to model real molecules (after all, equipotential surfaces of polyatomic molecules are never really convex) the model has the great advantage that it can be used to test thermodynamic perturbation theories on fluids of hard, convex bodies.

The Kihara potential was first proposed some 40 years ago [2] but it has most often been used to model not too dense gases, because the evaluation of the second virial coefficient can be performed analytically [3].

In the few last years there has been an increased interest in simulating convex hard-cores fluids in particular prolate spherocylinders [4, 5, 6], ellipsoids [7], discs [8]. However thus far only one simulation on non spherical convex particles interacting through a Kihara potential has been reported [9].

Boublik has proposed a perturbation theory for convex bodies interacting via a Kihara potential [10]. In the absence of simulation data this theory was compared with experimental data on N_2. However such a comparison is ambiguous because both the theory and the potential used are tested at the same time. Clearly a comparison of the theoretical predictions with the result of computer simulation using the same potential would be preferable. To this end we carried out numerical simulations of a system of rod-like particles interacting via a Kihara potential which can be regarded as an extension of the Lennard-Jones (12-6) potential to non-spherical cores.

Due to the fact that the properties of the reference system, both structural and thermodynamical, must be known in the perturbation scheme, we have simulated

† Permanent address: Physical Chemistry Department, Chemistry Faculty, Complutense University, 28040 Madrid, Spain.

the reference system (a soft repulsive model based on the WCA division for the Kihara potential), thus supplying information that may be used to improve the perturbation scheme.

A simulation at larger L/σ ($=L^*$) was also carried out in order to find the effects of the non-sphericity on the static correlation functions. Because Kihara potentials depend only on ρ, the shortest distance, the form of algorithm and the expressions for the evaluation of U and p as well as their tail contribution assuming uniform fluid for large values of ρ, are applicable to any (short-ranged) Kihara model, as long as the molecular core is convex.

2. Theoretical background

The Kihara (12–6) potential is given by the expression

$$\begin{aligned} u(\rho) &= 4\varepsilon \quad [(\sigma/\rho)^{12} - (\sigma/\rho)^6] \,, \quad \rho > 0 \,, \\ u(\rho) &= \infty \,, \qquad\qquad\qquad\quad \rho \leqslant 0 \,, \end{aligned} \tag{1}$$

where ε and σ are characteristic intermolecular parameters and ρ denotes the shortest distance between two convex bodies. Obviously $\rho(\mathbf{r}_{12}, \boldsymbol{\omega}_{12})$ is a function of the relative centre of mass vector $\mathbf{r}_{12}$ and the relative orientation of molecule 2 $\boldsymbol{\omega}_{12}$ once the orientation of molecule 1 has been fixed. Since the potential is a function of the shortest distance, it is useful to transform to variables characterizing the convex-body geometry. So rather than $\mathbf{r}_{12}$, the set θ, ϕ, and ρ is commonly used. In terms of these coordinates we can express $d\mathbf{r}_{12}$ as [11]:

$$d\mathbf{r}_{12} = \boldsymbol{\mu} \,.\, ((\delta \mathbf{r}_{12}/\delta\theta) \times (\delta \mathbf{r}_{12}/\delta\phi))\, d\theta\, d\phi\, d\rho \tag{2}$$

where $\boldsymbol{\mu}$ denotes the unit vector perpendicular to the supporting plane, and θ and ϕ are the polar angles of the supporting plane (see in Figure 1). Following Boublik's treatment we can express an average correlation function $g_{\mathrm{av}}(\rho)$ as

$$g_{\mathrm{av}}(\rho) = \frac{\int g(\rho, \theta, \phi)\boldsymbol{\mu} \,.\, ((\delta \mathbf{r}_{12}/\delta\theta) \times (\delta \mathbf{r}_{12}/\delta\phi))\, d\theta\, d\phi\, d\boldsymbol{\omega}_{12}}{\int \boldsymbol{\mu} \,.\, ((\delta \mathbf{r}_{12}/\delta\theta) \times (\delta \mathbf{r}_{12}/\delta\phi))\, d\theta\, d\phi\, d\boldsymbol{\omega}_{12}} \,. \tag{3}$$

The denominator in equation (3) is just $S_{c+\rho+c}$ the surface averaged over all the relative orientations, traced by the centre of one core when it moves around another core at constant distance ρ

$$S_{c+\rho+c} = \int \boldsymbol{\mu} \,.\, ((\delta \mathbf{r}_{12}/\delta\theta) \times (\delta \mathbf{r}_{12}/\delta\phi))\, d\theta\, d\phi\, d\boldsymbol{\omega}_{12} \,. \tag{4}$$

$S_{c+\rho+c}$ can be expressed in terms of a few simple geometrical quantities characterizing the convex bodies, the surface area S_c, and the mean radius of curvature of the respective cores R_c, and the distance ρ:

$$S_{c+\rho+c} = 2S_c + 8\pi R_c^2 + 16\pi R_c \rho + 4\pi\rho^2 \,. \tag{5}$$

The mean radius of curvature and the mean value of the 'excluded volume' generated using this procedure can be expressed in terms of S_c, R_c and V_c (volume of the convex core) [12]

$$R_{c+\rho+c} = 2R_c + \rho \,, \tag{6}$$

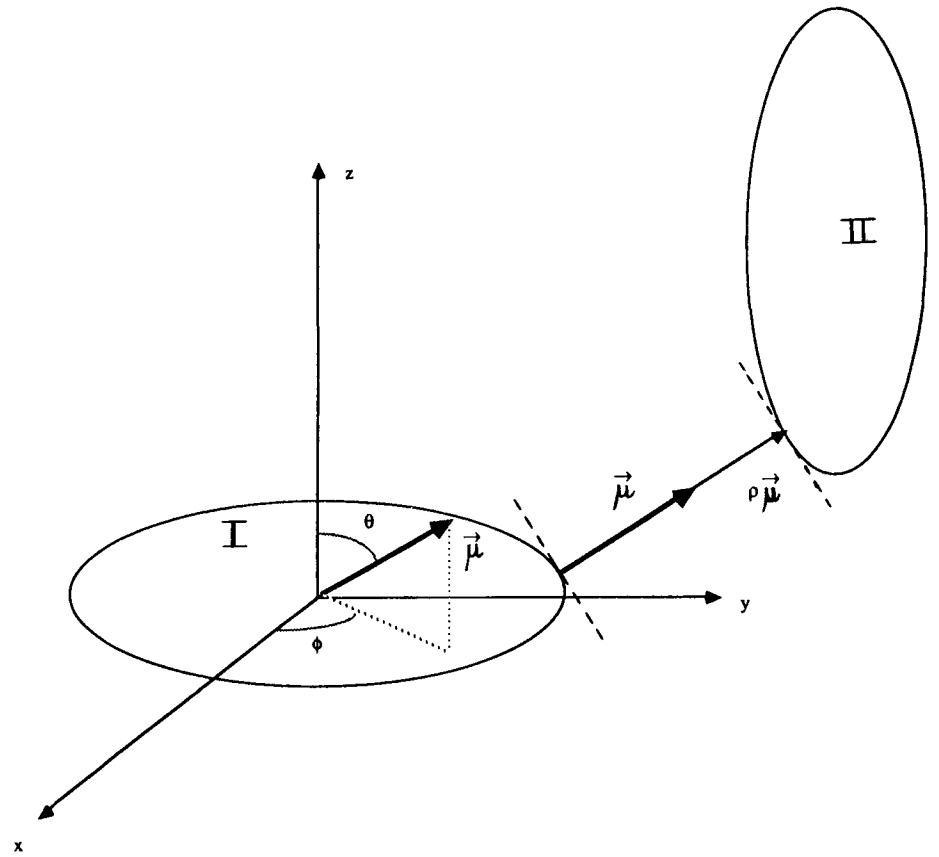

Figure 1. Visualization of the quantities that are used to specify the relative position and orientation of two convex bodies. Meaning of symbols: ρ, distance of closest approach between the two convex surfaces. $\boldsymbol{\mu}$, unit vector perpendicular to the supporting plane. (θ, ϕ), Polar and azimuthal angles specifying the orientation of $\boldsymbol{\mu}$ in a coordinate system fixed to molecule I.

$$V_{c+\rho+c} = (2V_c + 2S_c R_c) + (2S_c + 8\pi R_c^2)\rho + (8\pi R_c)\rho^2 + (4\pi/3)\rho^3 . \tag{7}$$

The excess internal energy can be expressed in terms of the average correlation function as [11]

$$U^{ex}/N = n/2 \int u(\rho) g_{av}(\rho) S_{c+\rho+c}\, d\rho \tag{8}$$

where n is the number density and N is the number of particles. Similarly the equation of state can be expressed in terms of the virial expression as [11]

$$Z = PV/NkT = 1 - 1/3NkT\langle \sum_{i<j} \sum \mathbf{r}_{ij} . \quad \nabla_{ij} u_{ij}(\rho_{ij})\rangle, \tag{9}$$

where the bracket means ensemble average and ∇_{ij} denotes the gradient operator. For a Kihara potential this gradient can be expressed easily as:

$$\nabla_{ij} u_{ij}(\rho_{ij}) = \boldsymbol{\mu}_{ij}(du_{ij}/d\rho_{ij}) . \tag{10}$$

The equation of state can be also written in terms of the average correlation function as

$$Z = 1 - n/6kT \int \langle \mathbf{r}_{12} \cdot \boldsymbol{\mu}_{12} \rangle_{\rho}^{\mathrm{en}} g_{\mathrm{av}}(\rho) S_{\mathrm{c}+\rho+\mathrm{c}}(du/d\rho)\, d\rho \tag{11}$$

where the bracket denotes ensemble average over all the configurations keeping the shortest distance between the cores constant. In the absence of structural correlations the evaluation of $\langle \mathbf{r}_{12} \cdot \boldsymbol{\mu}_{12} \rangle_{\rho}^{\mathrm{en}}$ reduces to a geometrical problem. For convex bodies:

$$\langle \mathbf{r}_{12} \cdot \boldsymbol{\mu}_{12} \rangle_{\rho}^{\mathrm{geo}} = \frac{3V_{\mathrm{c}+\rho+\mathrm{c}}}{S_{\mathrm{c}+\rho+\mathrm{c}}}. \tag{12}$$

The second virial coefficient of a Kihara-like potential is given by:

$$B_2(T) = 1/2\left(V_{\mathrm{c}+\mathrm{c}} - \int f(\rho) S_{\mathrm{c}+\rho+\mathrm{c}}\, d\rho \right) \tag{13}$$

where $f(\rho)$ denotes the Mayer function. This expression can be evaluated numerically or, for the Kihara (12–6) potential, analytically as a series of gamma functions.

Boublik [10] has proposed a perturbation scheme for fluids interacting through a Kihara (12–6) potential along the lines of the well-known WCA theory for simple liquids [21]. The potential is split into a reference part:

$$\left.\begin{aligned} u^0(\rho) &= u(\rho) + \varepsilon\,, \quad \rho < 2^{1/6}\sigma\,, \\ u^0(\rho) &= 0\,, \qquad\quad \rho > 2^{1/6}\sigma \end{aligned}\right\} \tag{14}$$

and a perturbation term:

$$\left.\begin{aligned} u^1(\rho) &= -\varepsilon\,, \quad \rho < 2^{1/6}\sigma\,, \\ u^1(\rho) &= u(\rho)\,, \quad \rho > 2^{1/6}\sigma\,. \end{aligned}\right\} \tag{15}$$

With this division a first order perturbation expansion can be formally written as follows:

$$A = A^0 + Nn/2 \int u^1(\rho) g^0(\mathbf{r}_{12}, \boldsymbol{\omega}_{12})\, d\mathbf{r}_{12}\, d\boldsymbol{\omega}_{12} \tag{16}$$

or using equation (3)

$$A = A^0 + Nn/2 \int u^1(\rho) g_{\mathrm{av}}^0(\rho) S_{\mathrm{c}+\rho+\mathrm{c}}\, d\rho. \tag{17}$$

It is clear now that a knowledge of $g_{\mathrm{av}}^0(\rho)$ is necessary for evaluating the first term of the perturbation expansion. For molecular liquids such as N_2, O_2 a reasonable choice for the core is to take a linear rod along the line joining the atomic centres. With this choice of the core, the geometrical parameter R_{c}, V_{c} and S_{c} take the values:

$$R_{\mathrm{c}} = L/4, \tag{18}$$

$$S_{\mathrm{c}} = 0, \tag{19}$$

$$V_{\mathrm{c}} = 0, \tag{20}$$

where L denotes the length of the linear rod.

3. Method

Simulations were carried out for the reference potential defined in equation (14) and for the Kihara potential equation (1) using linear rods as cores. During our simulation, a number of structural and thermodynamical properties were evaluated. These are briefly described below.

3.1. *Structural properties*

Let $\langle N(r)\rangle$ and $\langle N(\rho)\rangle$ denote the average number of pairs of molecules with a distance between the centre of mass between $(r - \Delta r/2, r + \Delta r/2)$, *respectively with a shortest distance between the cores lying in the range* $(\rho - \Delta\rho/2, \rho + \Delta\rho/2)$. Then $g(r)$ and $g_{av}(\rho)$ are computed as follows [13]:

$$g(r) = 2\,\frac{\langle N(r)\rangle}{Nn4/3\pi((r + \Delta r/2)^3 - (r - \Delta r/2)^3)}, \tag{21}$$

$$g_{av}(\rho) = 2\,\frac{\langle N(\rho)\rangle}{Nn(V_{c+\rho+(\Delta\rho/2)+c} - V_{c+\rho-(\Delta\rho/2)+c})}, \tag{22}$$

where r denotes the centre of mass distance, and ρ refers to the shortest distance. Typically, a value of $0{\cdot}04\sigma$ was chosen for both Δr and $\Delta\rho$.

The expansion in spherical harmonics of the pair correlation function for an isotropic system of linear molecules is given by [14]

$$g(r, \boldsymbol{\omega}_1, \boldsymbol{\omega}_2) = 4\pi \sum_{l, l', m} g_{ll'm}(r) Y_{lm}(\boldsymbol{\omega}_1) Y_{l'-m}(\boldsymbol{\omega}_2), \tag{23}$$

where $\boldsymbol{\omega}_1$ and $\boldsymbol{\omega}_2$ express the orientations of molecules 1 and 2 in a frame where $\mathbf{r}_{12}$ is along the z axis. The coefficients $g_{ll'm}(r)$ of this expansion were evaluated using the expression [15]

$$g_{ll'm}(r) = 4\pi g(r) \langle Y^*_{lm}(\boldsymbol{\omega}_1) Y^*_{l'-m}(\boldsymbol{\omega}_2)\rangle_{\text{shell}}, \tag{24}$$

where $\langle\ \rangle_{\text{shell}}$ denotes ensemble average over all the relative orientation with the distance between the centres of mass in the range $(r - \Delta r/2, r + \Delta r/2)$. In order to test whether the Monte Carlo averages were evaluated over isotropic equilibrium configurations the overall orientational order parameter of the systems was also calculated [16].

3.2. *Thermodynamical properties*

The excess internal energy U^{ex} and the equation of state (compressibility factor, (Z) were evaluated for the reference and the Kihara potential.

3.2.1. *Reference potential*

As this is a finite range potential, it does not pose special problems. The potential energy was evaluated during the runs and the pressure was calculated using the virial equation equation (9) together with equation (10).

3.2.2. *Kihara potential*

It seems clear that for the Kihara potential ρ is the natural variable to be used in any cutoff of the intermolecular interactions because the potential energy is a function of ρ only. Moreover, the tail contribution takes a simple form with this choice of the cutoff (equation (8) and equation (11)). We did the runs with a cutoff at $\rho_c = 2{\cdot}5\sigma$. As the oscillations of $g_{av}(\rho)$ were still appreciable at $\rho = 2{\cdot}5\sigma$, we used the actual values for the pair correlation function $g_{av}(\rho)$ obtained with $\rho_c = 2{\cdot}5\sigma$ for values of ρ up to $\rho = 3{\cdot}5\sigma$ and assumed uniform fluid for $\rho > 3{\cdot}5\sigma$. We verified that the numerical results for $g_{av}(\rho)$ were hardly affected when the cutoff value of the potential was increased from $2{\cdot}5\sigma$ to $3{\cdot}0\sigma$. The contribution of the tail was obtained assuming that:

$$g(\rho) = 1, \quad \rho > 3{\cdot}5\sigma. \tag{25}$$

Assuming a uniform fluid we can use $\langle \mathbf{r}_{12} \cdot \boldsymbol{\mu}_{12} \rangle_\rho^{geo}$ given by equation (12) instead of $\langle \mathbf{r}_{12} \cdot \boldsymbol{\mu}_{12} \rangle_\rho^{en}$ to obtain the tail correction to equation (11). It was observed that $g_{av}(\rho)$ typically differed less than 2 per cent, from the value of 1 beyond $\rho = 3{\cdot}5\sigma$. This provides an estimate of the relative error in the tail contribution.

The expression for the tail contribution to the internal energy and to the compressibility factor take the simple form:

$$U^{ex_{tail}}/N = n/2 \int_{\rho_{uni}}^{\infty} u(\rho) S_{c+\rho+c}\, d\rho \tag{26}$$

and

$$Z_{tail} = -n/(6kT) \int_{\rho_{uni}}^{\infty} (du/d\rho) 3 V_{c+\rho+c}\, d\rho. \tag{27}$$

In equations (26) and (27) ρ_{uni} denotes the first value of ρ in which uniform fluid can be assumed.

The tail contribution to the internal energy was about 2 per cent of the total value, and in the range (2–30 per cent) to the total pressure. The contribution of the 30 per cent was only obtained when the total pressure itself was close to zero.

4. Simulation conditions

A reference system of 108 rods with $L^* = 1$ and $T^* = T/(\varepsilon/k) = 1$ was studied at several values of the 'packing fraction', defined as

$$\eta = nV_c, \tag{28}$$

where V_c denotes the volume of a spherocylinder of σ diameter and length $L\sigma$ given by:

$$V_c = \pi\sigma^3/6(1 + 3/2L^*). \tag{29}$$

Also, a system of 216 linear rods at $T^* = 1{\cdot}075$ was studied for both the reference system and the Kihara fluid at several values of the packing fraction.

The L^* in the latter case was taken as $L^* = 0{\cdot}2899$ which follows from the parameter of N_2, $L = 0{\cdot}93$ Å and $\sigma = 3{\cdot}2072$ Å taken from [17]. We studied the isotherm for the reduced temperature $T^* = 1{\cdot}075$ because this allows us to compare

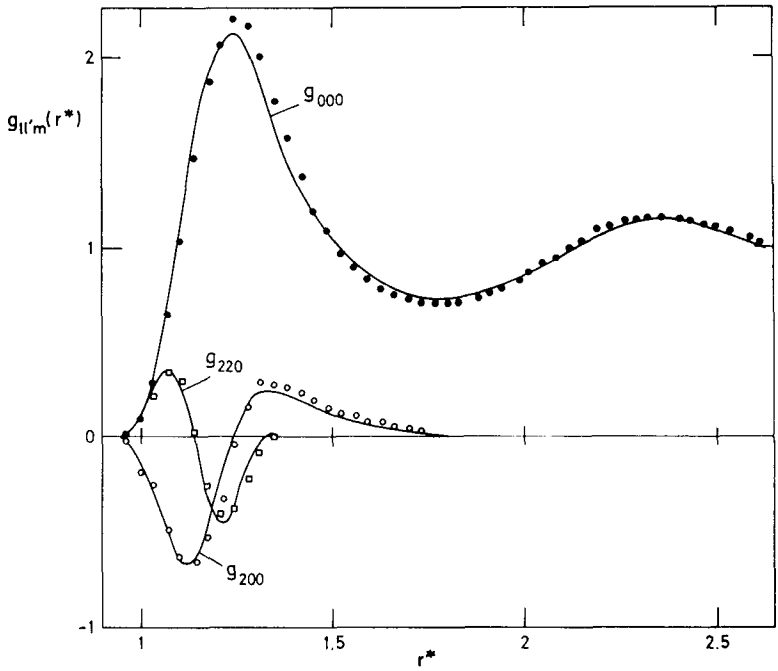

Figure 2. Spherical harmonics g_{000}, g_{200}, g_{220} for linear rods with $L^* = 0{\cdot}2899$ and $T^* = 1{\cdot}075$, at packing fraction $\eta = 0{\cdot}40$. Solid line shows the results of MC for the reference system. Dots and squares are the MC results for the Kihara potential ($r^* = r/\sigma$).

with two both the results of Boublik's theory [10] for this system and the experimental results for the N_2 at 126 K.

Constant volume Monte Carlo runs were carried out by the method of Metropolis *et al.* [18]. In all the simulations the initial configuration was a crystalline lattice of parallel linear rods in a cubical box. Periodic boundary conditions were used. New configurations in the MC run were generated by simultaneous random trial moves in both the position and the orientation of single molecules.

The number of configurations used for equilibration was usually about half million (= 5000 trial moves/particle for the 108 particle system) and thermodynamical averages were obtained over typically half million configurations sampling every 20 trial moves per particle. The acceptance ratio was always kept in the range (30–70 per cent). A typical run took about 4 hours of CPU time on a Cyber 990. An estimate of the statistical error was obtained by dividing the estimated standard deviation of the property under consideration by the number of independent samples. This latter quantity is defined as the number of samples divided by the 'correlation length'. This correlation length was estimated following [19].

As a test, a run was done with $L^* = 0$ which was in good agreement with results for the Lennard-Jones potential given in [20].

5. Results and discussion

The success of perturbation theories for simple liquids has clearly demonstrated that the repulsive forces are the determining factor for the fluid structure [21] at

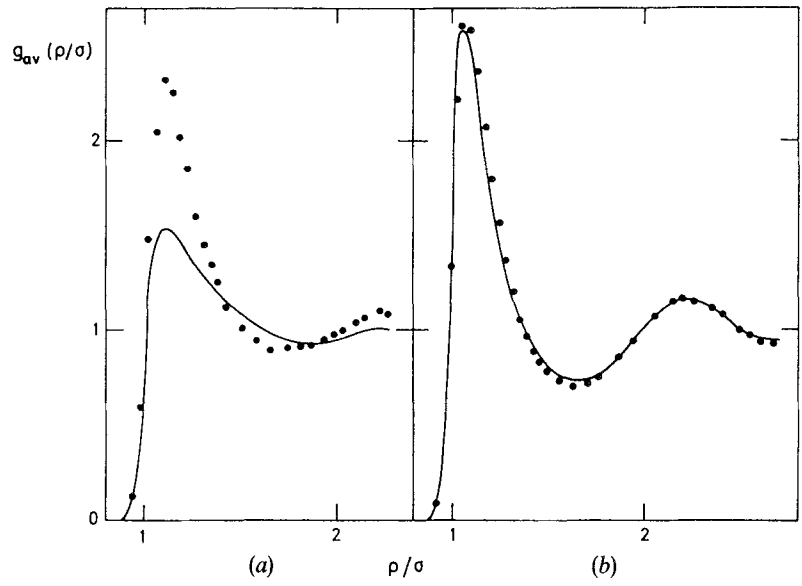

Figure 3. Average correlation function $g_{av}(\rho)$ for linear rods with $L^* = 0{\cdot}2899$ and $T^* = 1{\cdot}075$ for the reference potential (solid line) and for the Kihara potential (dots). (*a*) packing fraction $\eta = 0{\cdot}20$. (*b*) packing fraction $\eta = 0{\cdot}40$.

high densities. However, for molecular liquids is not, *a priori*, obvious that repulsive forces determine both the positional and orientational structure of a dense fluid. For molecules interacting with a Kihara potential, the reference system defined by the equation (14) contains all the repulsive forces, as is clear from equation (10). This division of the potential corresponds therefore to the WCA choice of the reference system. It would be interesting to know whether the structure of the reference system given by equation (14) reproduces the structure of the fluid interacting through the full Kihara potential given by equation (1).

In figure 2 the first 3 spherical harmonics of the expansion of the equation (23) are shown, for both the reference and the Kihara potential. It is clear from this figure that the positional structure g_{000} as well as the orientational one given by the g_{200}, g_{220} of the reference system are very close to those of the Kihara fluid, for the systems studied. Since all the thermodynamical properties of the Kihara fluid can be expressed in terms of the average correlation function $g_{av}(\rho)$ defined in equation (3), it is interesting to compare the behaviour of this average function for the reference and Kihara system. Such a comparison is shown in figure 3. This figure shows $g_{av}(\rho)$ for the reference potential and Kihara potential at two packing fractions ($\eta = 0{\cdot}20$ and $\eta = 0{\cdot}4$). At low densities the structure of the reference and Kihara system are seen to be quite different. This is to be expected as the low density limit of this correlation function is not the same for these two systems. However at high densities ($\eta = 0{\cdot}40$)$g_{av}(\rho)$ of the two systems is very similar. In fact, the resemblance between the $g_{av}(\rho)$ for the Kihara and reference fluid at $\eta = 0{\cdot}40$ is closer than that of the radial correlation function $g_{000}(r)$ (see figure 2 and figure 3(*b*)). Figure 3(*b*) provides information about the convergence of the perturbation series, which is given by equation (17) to first order. The Gibbs–Bogoliubov inequality applied to Kihara-

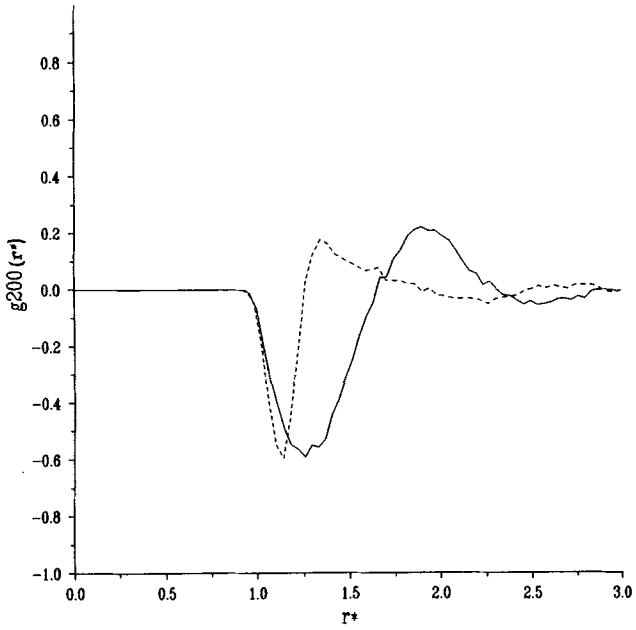

(*a*)

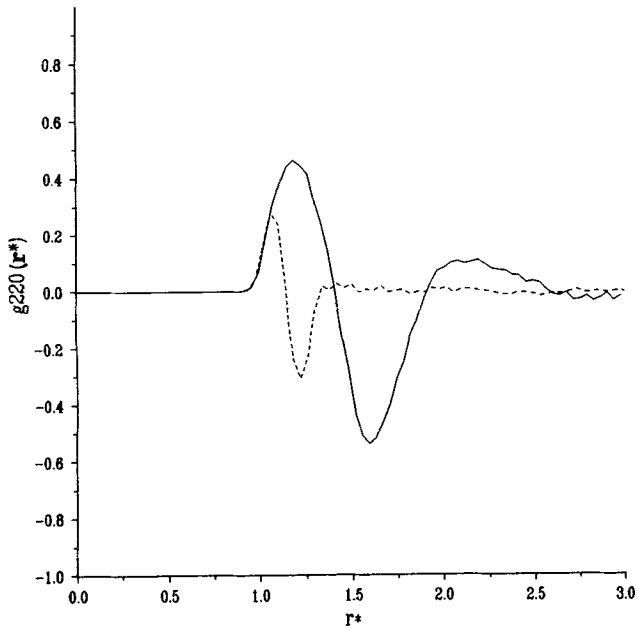

(*b*)

Figure 4. Spherical harmonics for a reference system with $I^* = 1$, $T^* = 1$ (solid line), and for a reference system with $I^* = 0{\cdot}2899$, $T^* = 1{\cdot}075$ (dashed line) both at a packing fraction $\eta = 0{\cdot}35$. ($r^* = r/\sigma$). (*a*) Spherical harmonic g_{200}. (*b*) Spherical harmonic g_{220}.

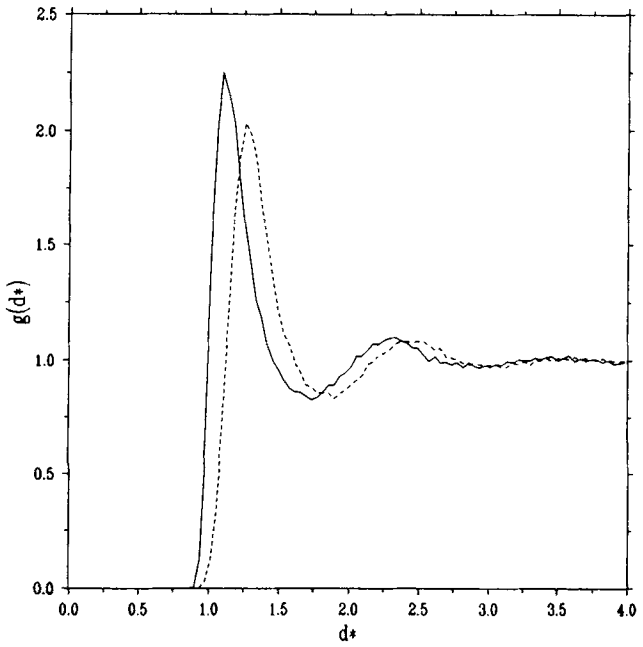

Figure 5. Average correlation function $g_{av}(\rho^*)$ (solid line) and radial distribution function $g(r^*)$ (dashed line) for the Kihara potential with $L^* = 0{\cdot}2899$, $T^* = 1{\cdot}075$ at packing fraction $\eta = 0{\cdot}25$, where d^* refers to both $\rho^*(\rho/\sigma)$ or $r^*(r/\sigma)$.

like potentials yields [14]:

$$A^0 + \frac{Nn}{2}\int u^1(\rho)g_{av}(\rho)S_{c+\rho+c}\,d\rho < A < A^0 + \frac{Nn}{2}\int u^1(\rho)g^0_{av}(\rho)S_{c+\rho+c}\,d\rho. \quad (30)$$

Clearly if $g_{av}(\rho)$ is similar to $g^0_{av}(\rho)$, as is shown in figure 3(*b*) then the perturbation expansion may be expected to converge rapidly and we may expect quite reasonable results by trunacting after the first-order term. Not surprisingly $g_{av}(\rho)$ is seen to be somewhat larger than $g^0_{av}(\rho)$ in the range where $u^1(\rho)$ is negative (cf. equation 30).

For more anisometric molecules where the orientational structure becomes stronger and longer ranged (see figure 4) the agreement between $g_{av}(\rho)$ and $g^0_{av}(\rho)$ is expected to be worse.

The relationship that exists between the average correlation functions $g(r) = g_{000}(r)$ and $g_{av}(\rho)$ is illustrated in Figure 5 where both are plotted for the reference system.

Let us continue with the analysis of the assumptions underlying in Boublik's perturbation theory. In Boublik's theory [10]

$$A^0_{res} = A_{res,\,ISPT^{HSP}(d_{BH})}, \quad (31)$$

where A^0_{res} refers to for the residual Helmholts free energy of the reference system and $A_{res,\,ISPT^{HSP}(d_{BH})}$ to the Helmholtz free energy of a hard equivalent system of spherocylinders (HSP) the diameter of which is computed using the BH criterion [22]

$$d = -\int f^0(\rho)\,d\rho. \quad (32)$$

Actually the free energy of the HSP is approximated by integration of an improved scaled particle theory (ISPT) equation of state. The free energy A may be

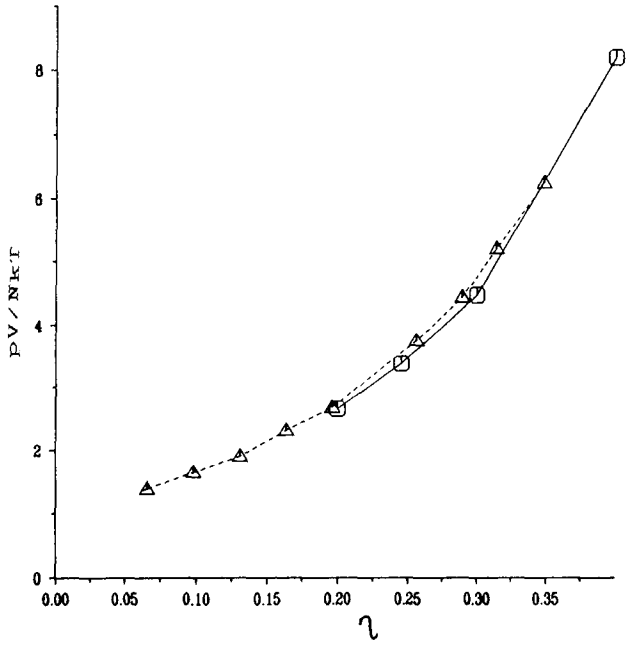

Figure 6. Compressibility factor for the reference system with $L^* = 1$ and $T^* = 1$ (dashed line) and for hard spherocylinders (solid line). The hard spherocylinder data were taken from reference [5].

obtained from the simulation by thermodynamic integration. However, here we only consider differential version of equation (31)

$$Z^0 = Z_{\text{ISPT}^{\text{HSP}}}(d_{\text{BH}}) \tag{33}$$

where the meaning of the symbols is the same as in equation (31). Z_{ISPT} is given by

$$Z_{\text{ISPT}} = 1/(1-\eta) + 3\alpha\eta/(1-\eta)^2 + \alpha^2\eta^2(3-\eta)/(1-\eta)^3, \tag{34}$$

$$\alpha = \frac{R_c S_c}{3V_c}. \tag{35}$$

Table 1. Simulation results of the compressibility factor Z_{sim} and excess internal energy $U^{\text{ex}}_{\text{sim}}$ for soft repulsive linear rods with $L^* = 1$ at $T^* = 1$. Z_{ISPT} stands for the compressibility factor of the reference system as given by Boublik approach of equation (33). Z_2 stands for the compressibility factor of the reference system as given by equation (36) with a Verlet–Weiss like choice of the hard spherocylinder diameter.

η	Z_{sim}	Z_{ISPT}	Z_2	$U^{\text{ex}}_{\text{sim}}/NkT$
0·065	1·37 ± 0·015	1·37	1·38	0·030 ± 0·001
0·098	1·62 ± 0·02	1·62	1·59	0·049 ± 0·002
0·131	1·90 ± 0·02	1·93	1·94	0·072 ± 0·001
0·164	2·31 ± 0·02	2·30	2·31	0·107 ± 0·002
0·196	2·67 ± 0·04	2·73	2·74	0·136 ± 0·004
0·256	3·75 ± 0·03	3·83	3·81	0·226 ± 0·004
0·289	4·45 ± 0·03	4·64	4·58	0·283 ± 0·003
0·314	5·21 ± 0·03	5·38	5·28	0·353 ± 0·003
0·348	6·25 ± 0·04	6·63	6·43	0·452 ± 0·004

Table 2. Simulation results of the compressibility factor Z_{sim} and excess internal energy U^{ex}_{sim} for soft repulsive linear rods with $L^* = 0{\cdot}2899$ at $T^* = 1{\cdot}075$. Z_{ISPT} stands for the compressibility factor for the reference system as given by Boublik approach of equation (33).

η	Z_{sim}	Z_{ISPT}	U^{ex}_{sim}/NkT
0·125	1·058 ± 0·003	1·055	0·00556 ± 0·00001
0·025	1·108 ± 0·005	1·113	0·0103 ± 0·0005
0·05	1·246 ± 0·007	1·242	0·024 ± 0·001
0·10	1·57 ± 0·01	1·56	0·055 ± 0·001
0·15	1·98 ± 0·02	1·98	0·095 ± 0·002
0·20	2·54 ± 0·03	2·53	0·150 ± 0·004
0·25	3·30 ± 0·03	3·28	0·226 ± 0·003
0·30	4·23 ± 0·03	4·30	0·320 ± 0·005
0·35	5·59 ± 0·03	5·73	0·460 ± 0·004
0·40	7·47 ± 0·04	7·76	0·661 ± 0·006

First we compare the behaviour of the compressibility factor Z of the reference system with $L^* = 1$ ($L^* = L/\sigma$) at several packing fractions with Z of a hard core system with $L^* = 1$ ($L^* = L/d$) where d is the hard diameter (see figure 6). The compressibility factor of these two systems is found to be nearly the same. The compressibility factor of the soft repulsive system is slightly larger than that of the hard system over the density range studied.

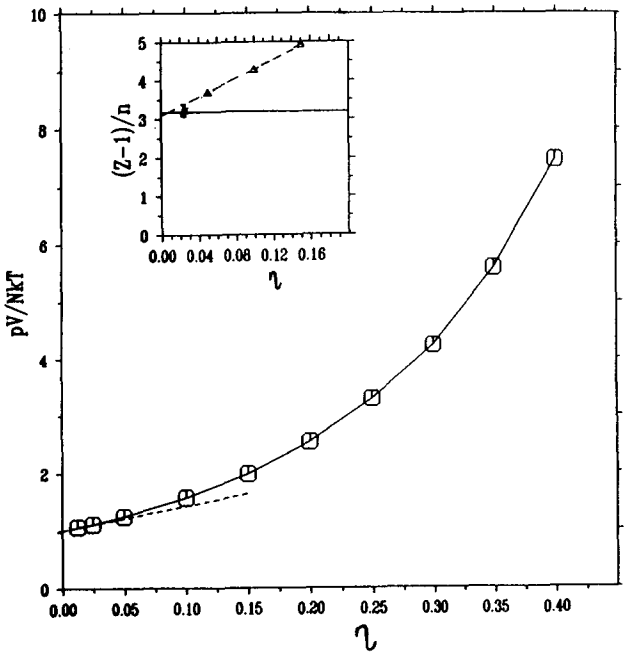

Figure 7. Compressibility factor for a reference system (solid line) with $L^* = 0{\cdot}2899$, $T^* = 1{\cdot}075$. The dashed line denotes the compressibility factor as given by the second virial coefficient of this system evaluated numerically from equation (13). The insert shows the behaviour of the function $(Z - 1)/n$ at low densities. The horizontal solid line indicates the value of the second virial coefficient. Note that a weighted least-squares fit to the MC data very nearly coincides with B_2 at $\eta = 0$.

The quality of the approximation expressed by equation (33) is shown in Tables 1 and 2. In these tables the present simulation results for the reference system are compared with the predictions based on equation (33) (Z_{ISPT}). It turns out that equation (33) works well for short rods at low and intermediate packing fractions, but less so at high densities and for less spherical particles. At high densities equation (33) overestimates the compressibility factor of the reference system. This effect is probably due to the fact that equations of state derived from scaled particle theory tend to overestimate the compressibility factor of hard core fluids. At high densities equation (31) leads therefore to an overestimate of the residual part of the Helmholtz free energy of the reference system. It has been suggested [23] that a better estimate of the compressibility factor of the reference system could be obtained using the following convex body equation of state [24]

$$Z = 1/(1-\eta) + 3\alpha\eta/(1-\eta)^2 + (3\alpha^2\eta^2(1-2\eta) + 5\alpha\eta^3)/(1-\eta)^3 \qquad (36)$$

together with a Verlet–Weiss like choice of the diameter of the hard spherocylinder [10]. The result of this approach is shown in the fourth column of table 1.

Figure 7 illustrates the simulation results of Z of the table 2. Note that for $\eta < 0{\cdot}05$, Z is adequately represented by the value computed using only the second virial coefficient. It is also found that, in this same density range, there is good agreement betwen the computed excess internal energy and the one calculated using the low density limit for $g_{\mathrm{av}}(\rho)$ (i.e. the Boltzmann factor).

Boublik assumes that $g^0_{\mathrm{av}}(\rho)$ is adequately described by $g^{\mathrm{HSP}}_{\mathrm{av}}(\rho)$ of a equivalent hard spherocylinder system. Of course it is interesting to know whether $g^0_{\mathrm{av}}(\rho)$ does in fact resemble $g^{\mathrm{HSP}}_{\mathrm{av}}(\rho)$. In figures 8 and 9 we compare these two functions for two different length-to-width ratios. The figures clearly demonstrate that the long-range

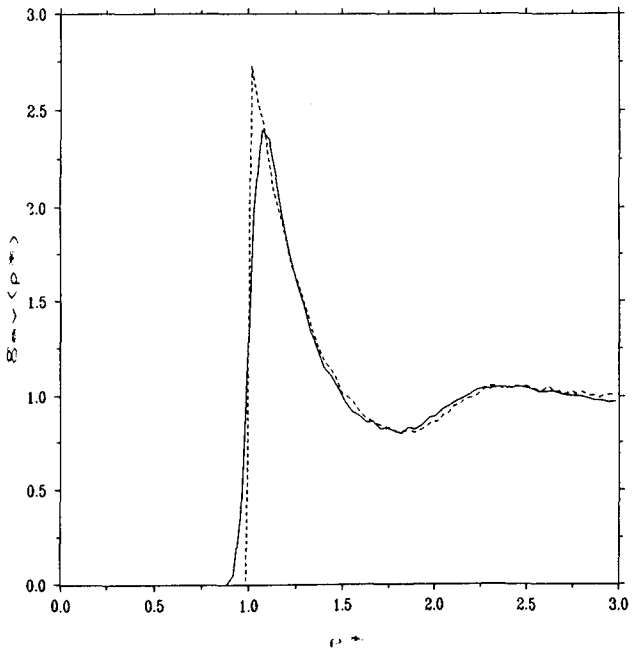

Figure 8. Comparison of $g_{\mathrm{av}}(\rho^*)$ for a reference system with $L^* = 1$ and $T^* = 1$ (solid line) and for a system of hard spherocylinders with the same L^* and at the same packing fraction $\eta = 0{\cdot}348$ (dashed line).

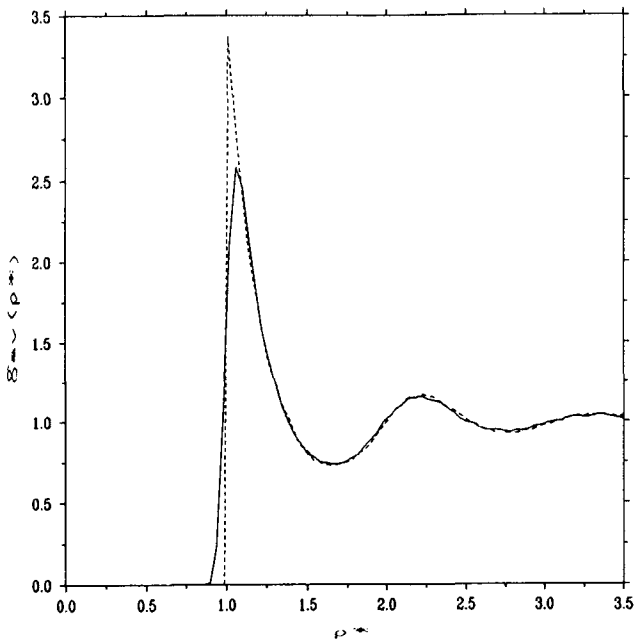

Figure 9. Comparison of $g_{av}(\rho^*)$ for a reference system with $L^* = 0{\cdot}2899$ and $T^* = 1{\cdot}075$ (solid line) and for a system of hard spherocylinders with the same L^* and at the same packing fraction $\eta = 0{\cdot}40$ (dashed line).

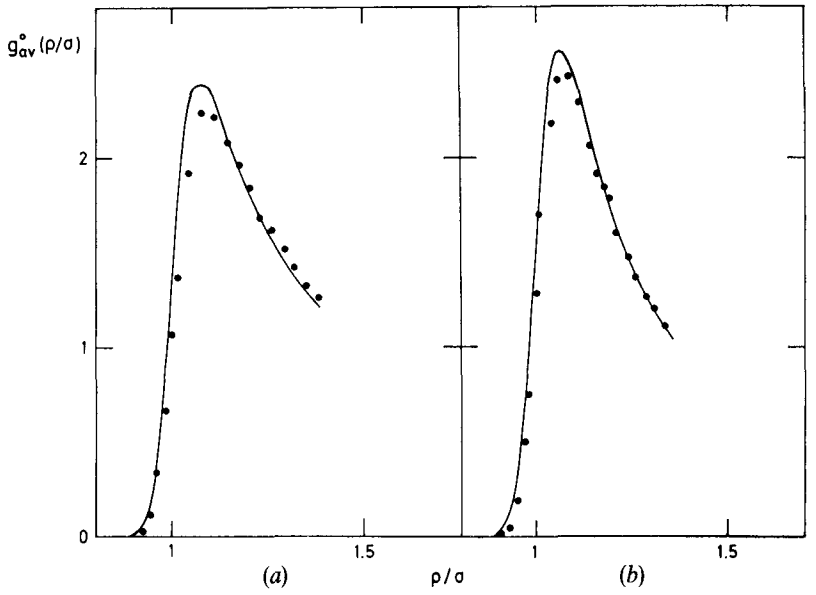

Figure 10. Average correlation function $g^0_{av}(\rho)$ of the WCA reference system. The solid line stands for the MC results and the dots for the zeroth order expansion of the function $y^0_{av}(\rho)$ (see text equation (37)). (*a*) For the $L^* = 1$ $T^* = 1$ and packing fraction $\eta = 0{\cdot}348$. (*b*) For the $L^* = 0{\cdot}2899$ $T^* = 1{\cdot}075$ and packing fraction $\eta = 0{\cdot}40$.

behaviour, of the WCA reference system and the corresponding hard-core system are almost equivalent, except for values of ρ around $\rho = \sigma$. However, as u^1 is constant for $\rho < 2^{1/6}\sigma$, the only thing that affects the value of the integral (equation (17)) in the range between $\rho = 0$ and $\rho = 2^{1/6}\sigma$, is the difference in the integrals of $g^0_{av}(\rho)$ and g^{HSP}_{av} in this range. Figures 8 and 9 suggest that although $g^0_{av}(\rho)$ and $g^{HSP}_{av}(\rho)$ may differ somewhat, there will be a strong cancellation of errors in the integral. It should be pointed out however that Boublik did not use simulation results for $g^{HSP}_{av}(\rho)$ but a semiempirical expression [10] which overestimates the value of $g^{HSP}_{av}(\rho = 0)$. This results in an underestimate of the integral in equation (17). As the sign of this error is opposite to the one introduced by using the approximate expression for A^0_{res} (equation (31)), one may expect an additional (fortuitous) cancellation of errors.

We have also tried to reproduce the results of $g^0_{av}(\rho)$ using a zeroth order expansion of the average background function $y^0_{av}(\rho)$ around the hard prolate spherocylinder system. The zeroth order expansion of $y^0_{av}(\rho)$ yields

$$g^0_{av}(\rho) = \exp(-\beta u^0(\rho)) y^{HSP}_{av}(\rho). \tag{37}$$

The results are shown in figure 10. The agreement is quite good, although in the two cases studied the zeroth order y expansion of $y^0_{av}(\rho)$ gives a lower first peak than the simulations results. Comparison of figures 8 and 9 with the figure 10 shows that the structure of the reference system (WCA type) is better reproduced by a zeroth order expansion of $y^0_{av}(\rho)$ around the hard spherocylinder system, than by the zeroth order expansion of $g^0_{av}(\rho)$ around the hard spherocylinder system.

In Table 3 we compare the results of Boublik's perturbation theory with the simulation data for the Kihara potential. The data in table 3 apply to a system with $L^* = 0{\cdot}2899$ (nitrogen. Figure 11 shows the computer compressibility factor for Kihara 'N_2' together with experimental data for real nitrogen from [25]. In the same figure we also show the predictions of Boublik's perturbation theory. From the figure it is clear that Boublik's theory is in fair agreement with the Monte-Carlo equation of state. The agreement is least satisfactory at low densities, as is to be expected for thermodynamic perturbation theories. This is understandable in view of the fact that the virial coefficient that follow from Boublik's theory is in disagreement with the exact expression equation (13). The agreement between the MC equation of state and experimental results is quite acceptable over the density range of packing fractions studied up to 3 $\rho_{critical}$. This result is not *a priori* obvious

Table 3. Simulation results of the compressibility factor Z_{sim} and excess internal energy U^{ex}_{sim} for Kihara linear rods with $L^* = 0{\cdot}2899$ at $T^* = 1{\cdot}075$. Z_{the} and U_{the} denote the results obtained with Boublik's theory [10].

η	Z_{sim}	Z_{the}	U_{sim}/NkT	U_{the}/NkT
0·05	0·70 ± 0·02	0·78	−0·664 ± 0·005	−0·40
0·10	0·44 ± 0·03	0·55	−1·24 ± 0·008	−0·84
0·15	0·30 ± 0·02	0·33	−1·79 ± 0·02	−1·33
0·20	0·27 ± 0·03	0·16	−2·27 ± 0·01	−1·85
0·25	0·16 ± 0·05	0·10	−2·76 ± 0·01	−2·41
0·30	0·24 ± 0·03	0·26	−3·27 ± 0·01	−2·99
0·35	0·75 ± 0·06	0·81	−3·80 ± 0·01	−3·57
0·40	1·74 ± 0·08	2·02	−4·34 ± 0·01	−4·12

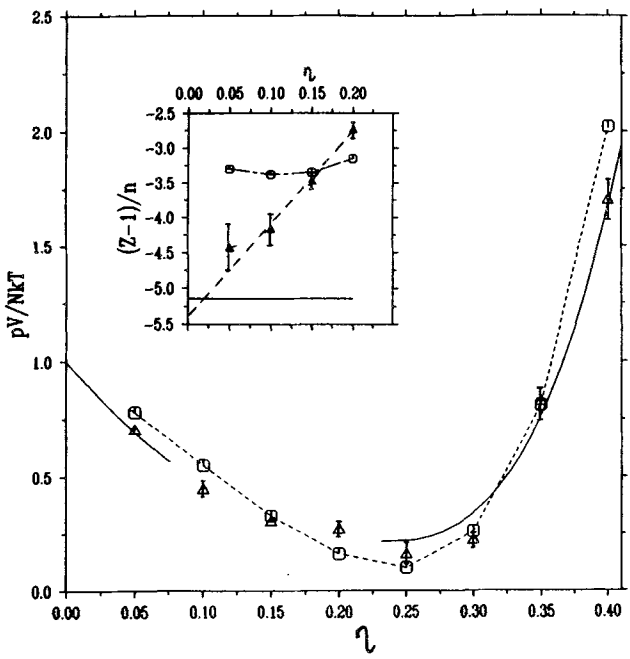

Figure 11. Compressibility factor of the N_2 at $T = 126$ K. Solid line: Experimental data taken from [25]. Squares: Boublik's perturbation theory. Triangles: Simulation results with the Kihara potential with $L^* = 0{\cdot}2899$ and $T^* = 1{\cdot}075$. The insert shows the low-density behaviour of the function $(Z-1)/n$ for this system. Triangles: Simulation results with the Kihara potential with $L^* = 0{\cdot}2899$ and $T^* = 1{\cdot}075$. Squares: Boublik's perturbation theory. Horizontal solid line: Second virial coefficient B_2 for the Kihara potential with parameters of [17] evaluated numerically from the equation (13). Note that a weighted least-squares fit to the MC data very nearly coincides with B_2 at $\eta = 0$.

because the Kihara potential parameters were fitted to second virial coefficient data only. Figure 12 shows the excess internal energy for N_2 and for the Kihara model as estimated by the perturbation theory and Monte Carlo simulation. It appears that the perturbation theory systematically predicts a higher value for this property than the simulations. At low packing fraction the simulation results approach the correct low density limit (as they should) but, again, the perturbation theory fails in this limit. The agreement between theory and the experimental data at higher densities is probably fortuitous, because the simulation results show that the Kihara potential actually underestimates the value of U^{ex}.

6. Conclusions

MC simulations have been carried out for systems interacting via a Kihara potential and a reference potential of the WCA type. For $L^* = 0{\cdot}2899$ ('N_2') it is clear that the repulsive forces determine the positional and orientational structure of the fluid at high densities. Furthermore for this length-to-width ratio, the perturbation WCA series appears to converge rapidly at high densities (this follows from figure 3(*b*) and equation (30)). This would justify the truncation of a WCA-like perturbation expansion after the first order term. Comparison of the simulation

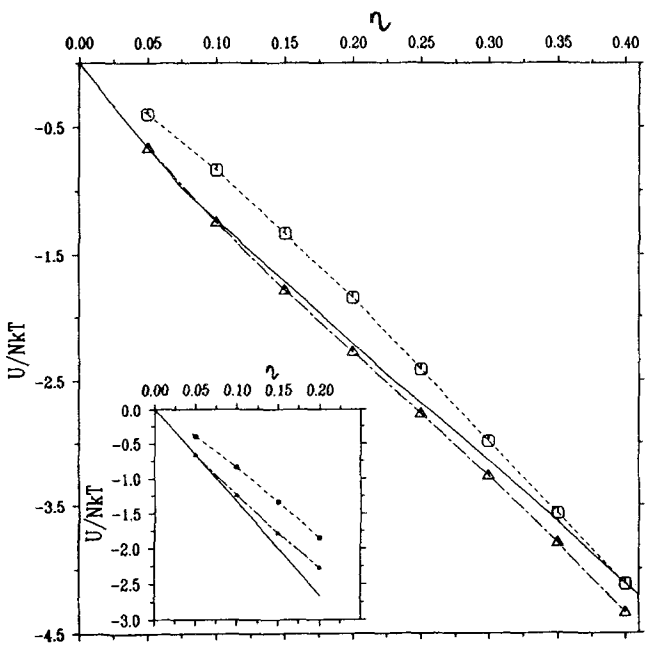

Figure 12. Excess internal energy of the N_2 at $T = 126$ K. Solid line: Experimental data taken from [25]. Squares: Boublik's perturbation theory. Triangles: Simulation results with the Kihara potential with $L^* = 0{\cdot}2899$ and $T^* = 1{\cdot}075$. The insert shows the behaviour of this quantity at low densities. Dashed line: Boublik's perturbation theory. Dashed–dotted line: Simulation results. Solid line: Estimate of U^{excess} given by equation (8) assuming the Boltzman factor for $g_{av}(\rho)$.

results with the results of a perturbation theory due to Boublik [10] shows fair agreement over a rather wide density range. The theory is found to be wanting in two respects. First of all, it appears that the Boublik theory overestimates A^0_{res} at high densities. Moreover this overestimate becomes worse as the length-to-width ratio of the molecule increases. The second problem with Boublik's theory is that it fails to give an accurate representation of $g^0_{av}(\rho)$ of the WCA reference fluid. Although this correlation function is very similar to $g^{HSP}_{av}(\rho)$ of a hard spherocylinder system for large values of ρ, the approximation clearly breaks down close to $\rho = \sigma$. The zeroth order expansion of the average background function of the WCA reference system $y^0_{av}(\rho)$ around a system of hard spherocylinders gives with high accuracy the structure of the reference fluid in the whole range of ρ values.

Comparison of the simulation results with experimental equation of state data for N_2 shows that the present Kihara potential reproduces the experimental results with acceptable accuracy over a much wider density range than it was designed for.

The work of the FOM Institute is part of the research program of FOM and is supported by the 'Nederlandse Organisatie voor Wetenschappelijk Onderzoek' (NWO). We thank to Dr. Boublik for reading the manuscript prior publication and for providing us with the data of the fourth column of table 1. One of us (C.V.) acknowledges the concession of a grant of the cultural agreement between Netherlands and Spain for carrying out this work and would like to thank N. Walet and F. Vitalis for computing help.

References

[1] LADANYI, B. M., and CHANDLER, D., 1975, *J. chem. Phys.*, **62**, 4308, and references therein.
[2] KIHARA, T., 1951, *J. phys. Soc. Japan.*, **16**, 289.
[3] MASON, E. A., and SPURLING, T. H., 1969, *The Virial Equation of State* (Pergamon Press).
[4] VIEILLARD-BARON, J., 1974, *Molec. Phys.*, **28**, 809.
[5] MONSON, P. A., and RIGBY, M. 1978, *Chem. Phys. Lett.*, **58**, 122.
[6] BOUBLIK, T., NEZBEDA, I., and TRNKA, O. 1976, *Czech. J. Phys.* B, **26**, 1081.
[7] FRENKEL, D., and MULDER, B. M., 1985, *Molec. Phys.*, **55**, 1171.
[8] DESTRADE, C., FOUCHET, P., GASPAROUX, H., TINH, N. H., LEVELUT, A. M., MALTHETE, J., 1984, *Molec. Crystals liq. Crystals*, **106**, 121.
[9] KANTOR, R., and BOUBLIK, T. *Czech. J. Phys.* (in the press).
[10] BOUBLIK, T., 1976, *Molec. Phys.*, **32**, 1737.
[11] BOUBLIK, T., 1974, *Molec. Phys.*, **27**, 1415.
[12] BOUBLIK, T., and NEZBEDA, I., 1986, *Czech. chem. Commun.*, **51**, 2307.
[13] BOUBLIK, T., NEZBEDA, I., 1976, *Czech. J. Phys.* B, **26**, 1081.
[14] HANSEN, J. P., MCDONALD, I. R., 1986, *Theory of Simple Liquids* (Academic Press).
[15] STREETT, W. B., and TILDESLEY, D. J., 1976, *Proc. R. Soc.* A, **348**, 485.
[16] EPPENGA, R., and FRENKEL, D., 1984, *Molec. Phys.*, **52**, 1303.
[17] KOIDE, A., and KIHARA, T., 1974, *Chem. Phys.*, **5**, 34.
[18] METROPOLIS, N., ROSENBLUTH, M. N., ROSENBLUTH, A. W., TELLER, A. H., and TELLER, E., 1953, *J. chem. Phys.*, **21**, 1087.
[19] JACUCCI, G., RAHMAN, A., 1984, *Nuovo Cim.*, **4**, 347.
[20] HANSEN, J. P., and VERLET, L., 1969, *Phys. Rev.*, **184**, 151.
[21] WEEKS, J. D., CHANDLER, D., and ANDERSEN, H. C., 1971, *J. chem. Phys.*, **54**, 5237.
[22] BARKER, J. A., HENDERSON, D., 1967, *J. chem. Phys.*, **47**, 4714.
[23] BOUBLIK, T. (private communication).
[24] BOUBLIK, T., 1981, *Molec. Phys.*, **42**, 209.
[25] JACOBSEN, R. T., and STEWART, R. B., 1973, *J. phys. Chem. ref. Data*, **2**, 757.